MŰEGYETEM 1782

TDK THESIS

Development of a nonconventional electron spin resonance spectrometer

Balázs Gyüre

Thesis supervisor: Ferenc Simon (BME Department of Physics)

Budapest University of Technology and Economics

BME
2014.

Contents

Acknowledgment

1 Introduction and motivation

High sensitivity spectrometers are essential tools of modern solid state physics research. Many problems have arisen in the ESR laboratory of the BME Physics Institute that require the improvement of the available electron spin resonance (ESR) spectrometers. In our cooperation with a solid state physics laboratory of CSIC (Spanish National Research Council) we have realized the necessity of the development of a high magnetic field ESR, in which low temperatures can be reached.

Conventional ESR set-ups typically work at $9\,\mathrm{GHz}$ frequency. Keeping the $g \approx 2$ g-factor of non-interacting electrons in mind, the magnetic field used is $0.32\,\mathrm{T}$. The temperature range is 4.2-300 K. The cryostats are usually of the flow-through design with a huge helium consumption. However, these conditions are not adequate for the study of correlated magnetic systems, e.g. ferromagnetic and antiferromagnetic materials. Therein, high magnetic fields (-9 T), while using the 9 GHz frequency range and temperatures below 4 K would be beneficial in the examination of these materials. Using such an ESR, frequency-magnetic field ranges could be reached, not available in any other spectrometer. An example is shown in Fig. 1, where the highly non-linear $B - f$ ESR modes are shown for the MnF_2 antiferromagnet.

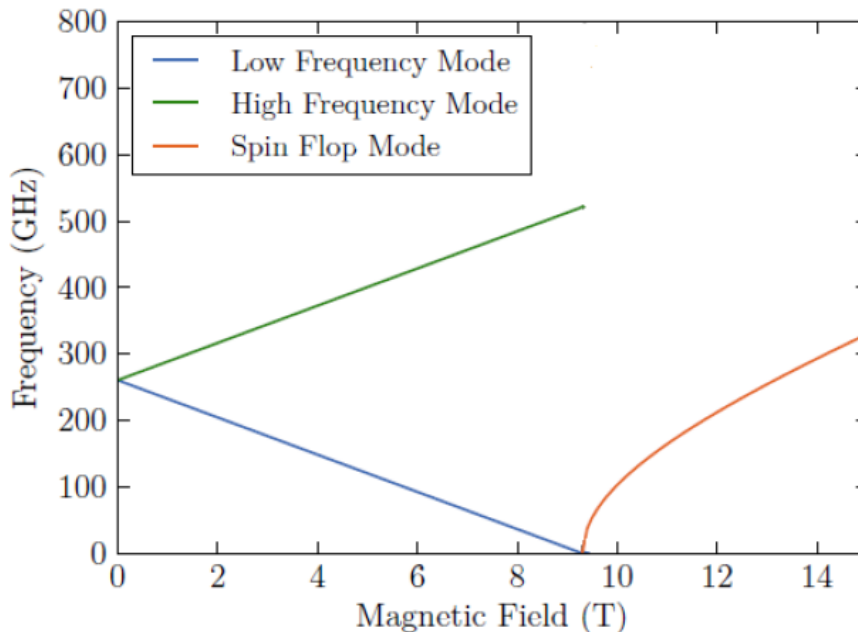Figure 1: The ESR resonance modes for the MnF_2 antiferromagnet after Ref. [1]. Note the presence of a resonance at high magnetic field (9 T) for a 9 GHz excitation.

The low temperature and high magnetic field is available in the cryostat of superconducting magnets, however in these cryostats the small space does not allow the use of traditional microwave cavities, which is an essential part of ESR spectrometers. To solve

this problem, I have built a probehead, which uses a so called loop-gap resonator. Loop-gap resonators correspond to the so-called lumped microwave resonators, i.e. therein no microwave standing wave is sustained, instead an inductor (the loop) and a capacitor (a gap) form an RLC circuit. As a result, loop-gap resonators are of much smaller scale than the conventional cavities at the same frequency. I present the basics of ESR spectrometers, the design of the probehead, the problems during its construction and use, and the measurements demonstrating its functionality.

2 Theoretical basics

2.1 Electron Spin Resonance spectrometer

2.1.1 Basics of ESR Spectroscopy

The ESR spectrometry is based on paramagnetic resonance. As it is a non-contact method, it may be used to study air sensitive samples.

An ESR spectrometer studies the transition between the spin states in high magnetic fields. When an unpaired electron is placed in a high magnetic field, it's two spin states have different energy levels. The energy of the transition between these two states is provided by the absorption of a microwave photon.

$$\hbar\omega = \Delta E = g_e \mu_B B \tag{1}$$

where g_e is the g-factor of the electron, $\mu_B = 9.27 \cdot 10^{-24}$ J/T is the Bohr-magneton.

By applying a constant frequency microwave radiation and sweeping the magnetic field, the absorption of the studied material can be measured.

2.1.2 Block diagram of an ESR spectrometer

Many types of ESR spectrometers may be realized, two are presented herein. To measure the reflection from an ESR resonator, we need a microwave component that separates that microwave radiation coming from the source and the the radiation coming from the resonators. This may be a circulator or a 180 degree hybrid, a so-called magic tee. To measure the microwave voltage, an RF mixer is used.

Fig. 2 shows the block diagram of a spectrometer using a circulator. The microwave mixer used requires 7 dBm microwave power on its LO port and the maximum power on its RF port must be 0 dBm. A directional coupler is used to split the microwave power between the LO port and the measurement. The phase shifter before the LO port may be omitted if an IQ mixer is used. The magnetic modulation is driven by the output of the lock-in amplifier. To achieve -the sometimes necessary- high magnetic modulation, an amplifier with large current output may be used. The large DC magnetic field is commonly achieved by a superconducting magnet. To satisfy the Bloch-equations describing the absorption, the large static magnetic field should be perpendicular the magnetic field component of the microwave in the resonator.

See Fig. 3 for a spectrometer using a 180 deg hybrid. To dissipate the energy returning to the source from the resonator an isolator is used. Note that the energy at the RF port of the mixer could be at most 4 dBm, but there is at least 4 dB loss on the cables, so there is no danger of damaging the mixer.
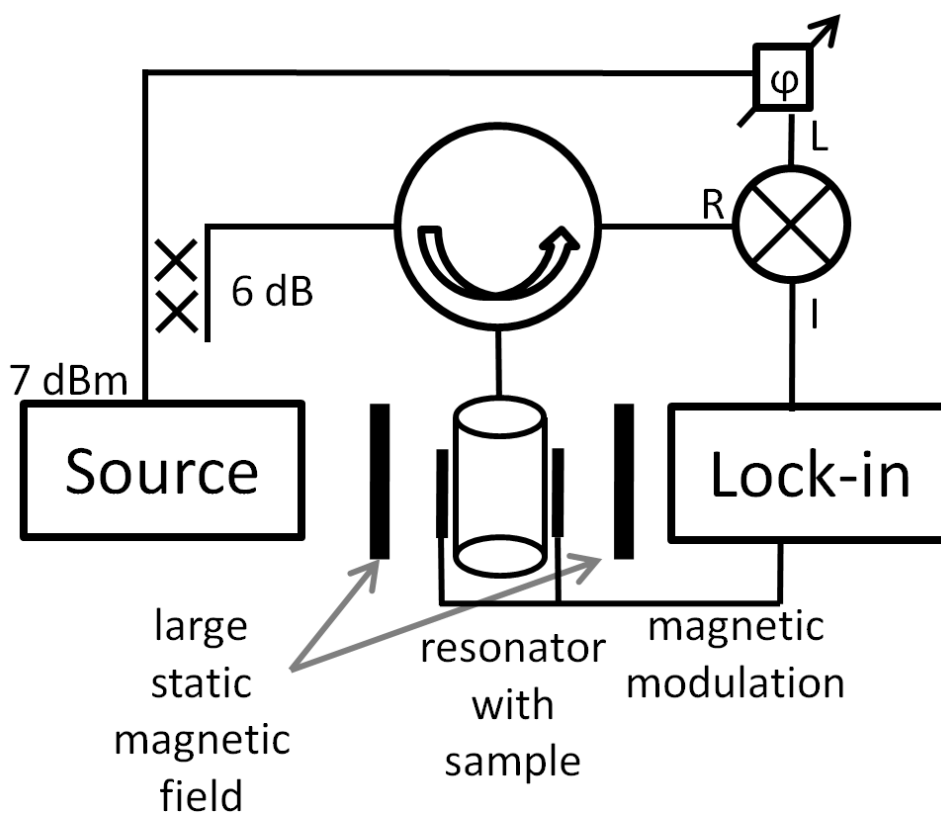
6

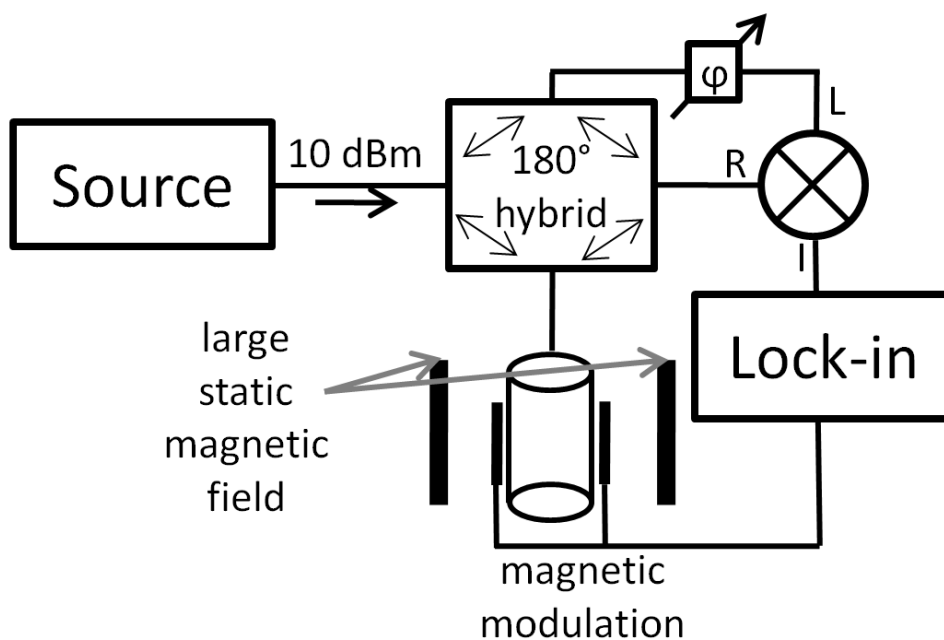Figure 2: Block diagram of the ESR spectrometer incorporating a circulator.

Figure 3: Block diagram of the ESR spectrometer using a 180 degree hybrid coupler.

2.1.3 Operation of ESR spectrometers

The sample is placed in a microwave resonator. The magnetic field is swept in a course of a few minutes and modulated at the frequency of about $100\,\mathrm{kHz}$. The reflection from the microwave resonator is measured by a microwave mixer with its IF port connected to a lock-in amplifier. The magnetic modulation is driven by the internal oscillator of the lock-in amplifier and amplified to achieve higher current and higher modulation.
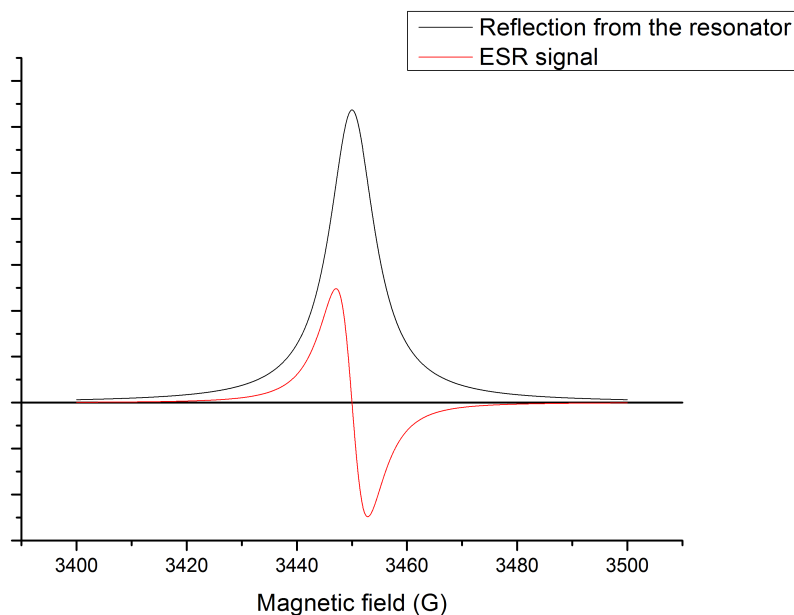

Figure 4: A typical reflection from the microwave resonator and the measured ESR signal.

The absorption of a typical sample when the magnetic field is swept is a Lorentzian. The change in the absorption of the sample changes the reflection from the microwave resonator. Due to the magnetic field being modulated, the measured signal is the first derivative of the Lorentzian (see Fig. 4).

2.2 Basics of the microwave cavity

An RLC circuit made of lumped elements cannot be simply used in the microwave frequency-domain, so instead, a cavity may be used as a resonator, whose walls are made of a highly conductive material, usually copper. The dimensions of the cavity are comparable to the wavelength of the microwave radiation. Excited on its resonance frequency, a cavity can sustain a standing wave mode, which is the superposition of the waves reflected from the cavity walls. A cavity is capable of maintaining several modes, whose properties are based on the shape and size of the cavity. A large microwave field builds up when it is coupled to a waveguide. When coupling to the cavity, care must be taken to match the desired mode in the cavity to the mode in the waveguide. [2]
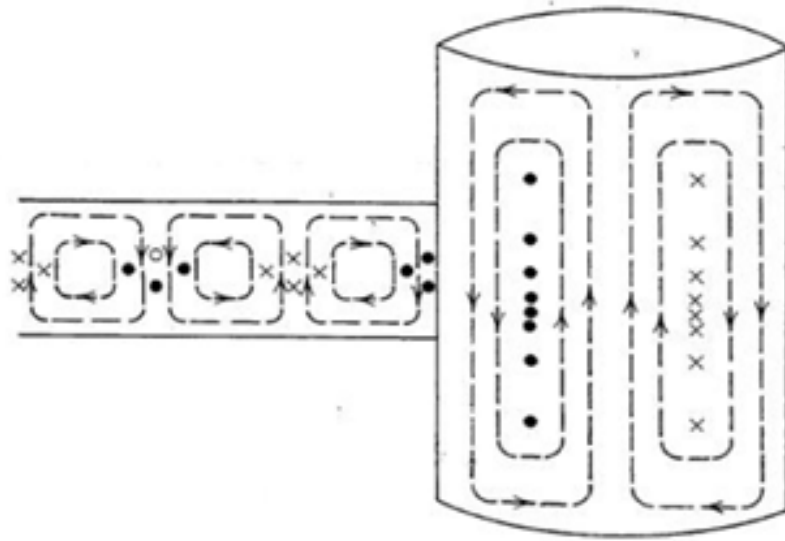

Figure 5: Electromagnetic field in the cavity and the waveguide (dashed line: magnetic field, continuous line: electric field) [2].

It is generally known that the quality factor (Q) sets the magnitude of the electromagnetic field in the cavity in the stationary state.

$$Q = 2\pi \frac{\text{stored energy in the system}}{\text{dissipated energy per period}} = \frac{f_0}{\Delta f} \tag{2}$$

f_0 is the resonance frequency, Δf is the full width at half maximum (FWHM) of the resonance curve. Using this relation between the Q factor and the FWHM is the most widely used method of measuring the Q factor.

The Q factor of a cavity depends on the physical properties of the cavity, any sample placed in it and the coupling [2].

$$\frac{1}{Q} = \frac{1}{Q_{\text{empty cavity}}} + \frac{1}{Q_{\text{sample}}} + \frac{1}{Q_{\text{coupling}}} \tag{3}$$

$$\frac{1}{Q} = \frac{1}{Q_0} + \frac{1}{Q_{\text{coupling}}} \tag{4}$$

Q is the quality factor for the whole system and Q_0 for the cavity without the coupling taken into account (uncoupled cavity). $Q_{\text{empty cavity}}$ is also called unloaded cavity. Critical coupling is achieved when there is no reflection from the cavity in the stationary state. It can be shown that in this case $Q_{\text{coupling}} = Q_0$.

2.2.1 Loop-gap resonator

During the design of the probeheads the need for smaller than regular resonator was realized. One solution is the so-called loop-gap resonator. A loop-gap resonator is an alternative of the regularly used cylindrical resonators, it may be considered to resemble a resonator made of classic lumped circuit elements.
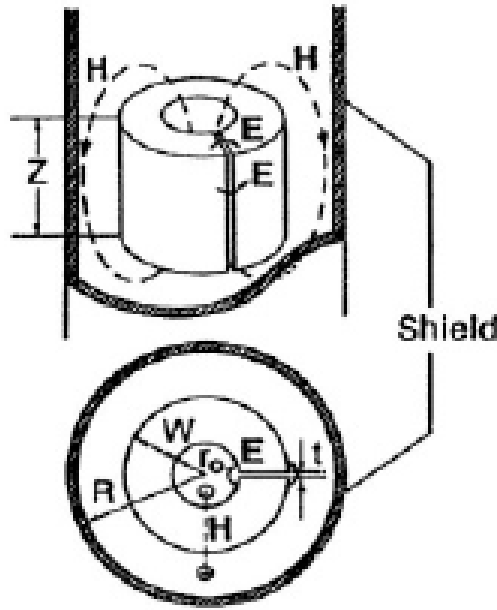

Figure 6: Schematics of a 1-loop 1-gap resonator. From Ref. [3].

A 1-loop 1-gap resonator consists of a conductor loop, which contains the magnetic field, and a gap in this loop, containing the displacement current (Fig. 6). A microwave shield is required for two reasons: to contain the return flux and to prevent radiative loss.

A 2-loop 1-gap resonator consists of two circular holes and a thin gap connecting them (Fig. 7). Note that within a classic cavity resonator the electromagnetic field may be considered as a standing wave in a waveguide, while in a loop-gap resonator the electric and magnetic fields are more spatially separated, as there is only a small electric field within the loops and only a small magnetic field within the gap. The dimensions a loop-gap resonator may be much smaller than the resonant wavelength. In a 2-loop 1-gap resonator the return flux is contained without a shield, but the shield is still needed to prevent radiation.

To calculate the resonance frequency of the resonator, the 2 loops should be considered coils and the gap should be considered a capacitor. We use the notation of the dimensions
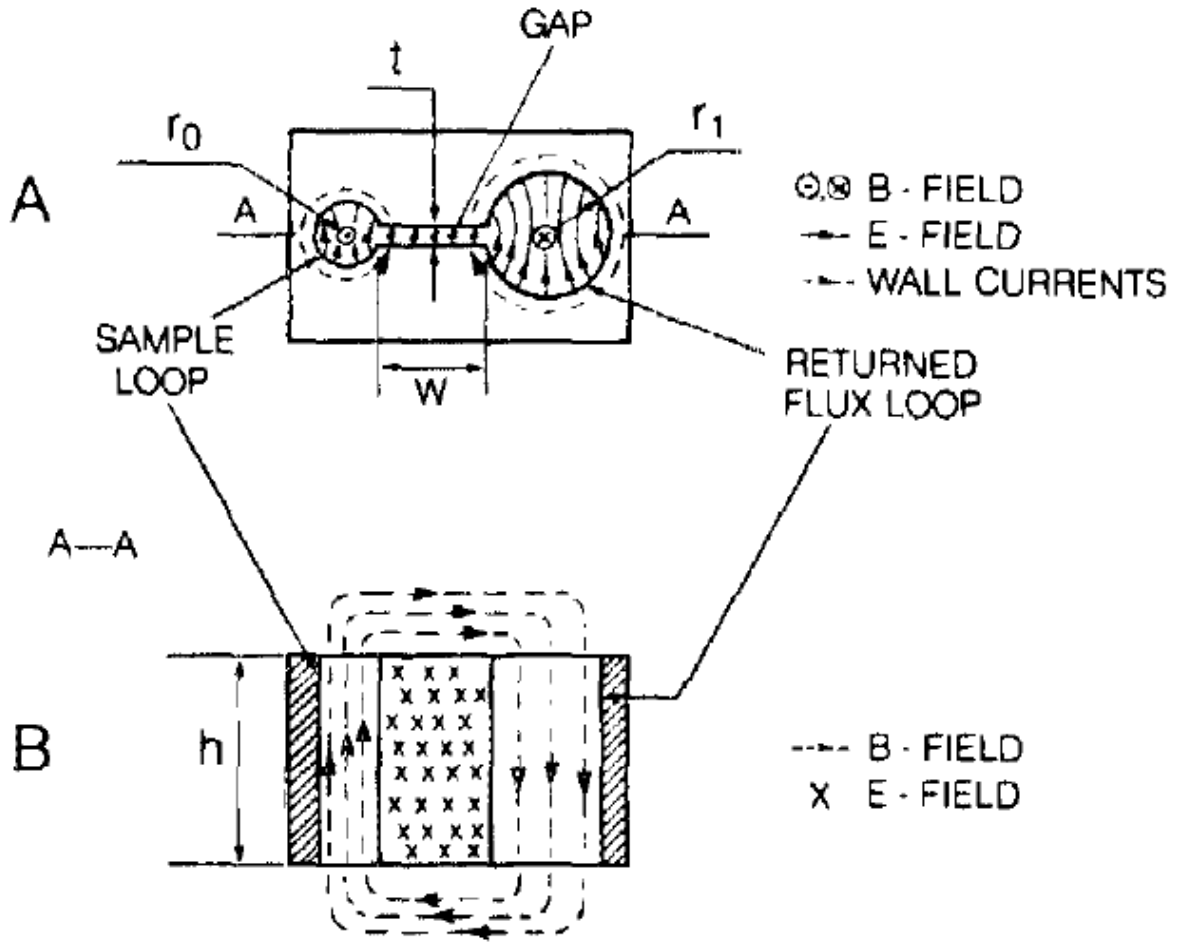
Figure 7: Schematics of a 2-loop 1-gap resonator. r_0 and r_1 are the radii of the loops, W is length, t is the separation of the gap. h is the depth of the resonator. From Ref. [4].

given in Fig. 7.

$$C = \epsilon h W / t \tag{5}$$

$$L = \mu \pi r^2 / h \tag{6}$$

$$f_0 = \frac{c}{2\pi} \left(\frac{t \left(1/r_0^2 + 1/r_1^2 \right)}{\pi \kappa W} \right)^{1/2} \tag{7}$$

where c is the speed of light, and κ is the dielectric constant.

It was found that this calculation only yields approximate results, as it does not consider the magnetic field outside the loops and electric field outside the gap. Reference [4] shows that if we consider these electromagnetic fields, we arrive at a much more precise value for the resonance frequency. For our purposes however it is sufficient to know that the calculated values are about 30% too high. Once the loop-gap resonator is manufactured, an empirical test yields the accurate resonance frequencies.

Loop-gap resonators yield a lower quality factor than their cylindrical counterparts. A cylindrical resonator made of copper generally has a quality factor of a few thousand,

11

while a loop-gap generator generally has a quality factor of a few hundred. This is due to the smaller surface of the loop-gap resonator where the microwave sustaining crrent flows. In comparison however, as a loop-gap resonator is much smaller, the filling factor is much larger for the same sample. The filling factor measures the amount of magnetic field, which penetrates the sample, so a higher filling factor may increase the ESR signal and thus compensate for the lower Q.

Normally automatic frequency control (AFC) is needed to keep the the frequency of the microave source on the resonance frequency of the resonator. Having a lower Q also has the advantage that it is not necessary to use an AFC circuit in the ESR setup.
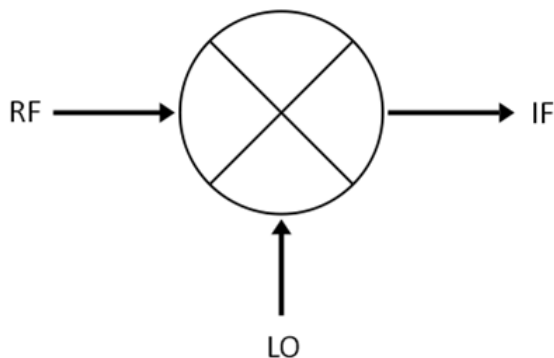
2.3   Microwave mixer

Figure 8: Schematics of a microwave mixer. LO, RF, and IF denote the local oscillator, radio and intermediate frequency ports, respectively.

The mixer is a widely used device in electronics. It achieves the phase sensitive mixing of two AC voltage signals and are found in practically all RF and microwave communication devices. In the ESR spectrometer technology, the use of mixers is vital as it achieves the high sensitivity detection of microwaves.

The use of radio frequency signals in telecommunications would require a broadband instrument given that information is transmitted over several frequency channels. The idea of mixing is to keep the need for broadband circuitry for a minimum and to use the same frequency (the IF) wherever possible. For measurements at lower frequencies the high frequency signals must be downmixed to the frequency of the instruments. This is achieved by a mixer.

$$f_{\mathrm{IF}} = f_{\mathrm{RF}} \pm f_{\mathrm{LO}} \tag{8}$$

Using two signals with different frequencies, we get a signal whose frequency is the difference between the two incoming frequencies. When used as a downconverter, the local oscillator (LO) input is a signal with a constant power and high frequency and the RF is the signal we wish to measure, whose magnitude is significantly smaller than the LO signal. The output is generated on the IF port.

This mixing of signals is achieved by multiplying the AC voltages of the two signals:

$$V_{\mathrm{LO}} = A_{\mathrm{LO}} \cos(\omega_{\mathrm{LO}} t) \tag{9}$$

$$V_{\mathrm{RF}} = A_{\mathrm{RF}} \cos(\omega_{\mathrm{RF}} t + \Phi) \tag{10}$$

$$V_{\mathrm{IF}} = C V_{\mathrm{LO}} V_{\mathrm{RF}} \tag{11}$$

$$V_{\mathrm{IF}} = \frac{K A_{\mathrm{LO}} A_{\mathrm{RF}}}{2} \cos[(\omega_{\mathrm{RF}} - \omega_{\mathrm{LO}})t + \Phi)] + \frac{K A_{\mathrm{LO}} A_{\mathrm{RF}}}{2} \cos[(\omega_{\mathrm{RF}} + \omega_{\mathrm{LO}})t + \Phi)] \tag{12}$$

where C is a constant and is characteristic for a mixer. As it can be seen, both the sum and difference of LO and RF frequencies can be observed in the IF port.

Mixers use the non-linear nature of diodes to achieve the multiplication of two signals. Multiple diode configurations can be used to cancel out the unwanted signals, and decrease noise. These configurations are shown in Fig. 9 and Fig. 10. The so-called double balanced mixer has higher power and frequency ranges than single balanced mixers.
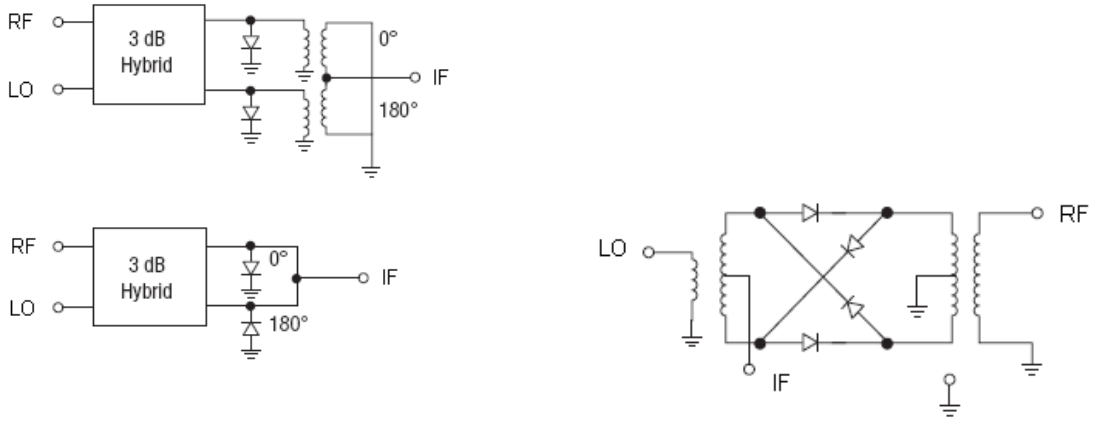

Figure 9: Schematics of common single balanced mixers. Note that the IF is generated either by subtracting the DC component directly or by using transformers. From Ref. [5].

Figure 10: Schematics of a common double balanced mixer. From Ref. [5].

When the LO and RF signals have the same frequency, the IF signal becomes a DC voltage, whose magnitude is independent of the LO signal amplitude, proportional to the RF signal amplitude and to cosine of the phase between these two signals. However, when the phase between the RF and LO signals is 90°, we do not measure a signal in the IF output.
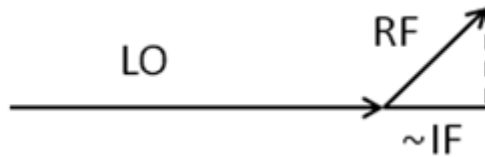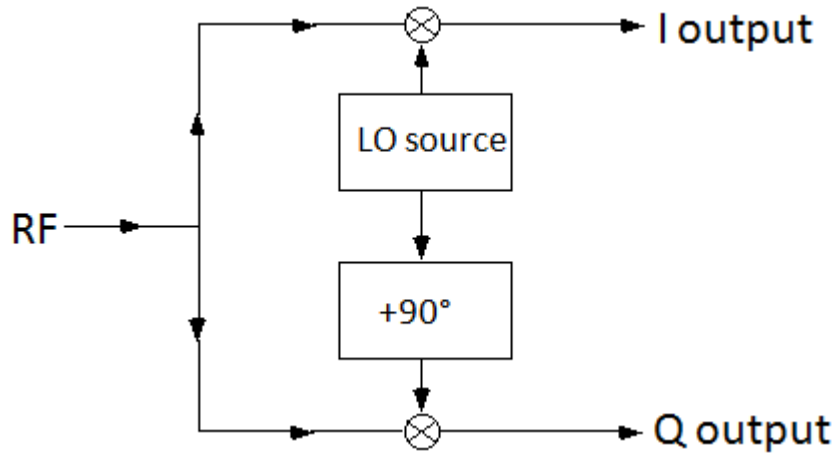

Figure 11: DC output of a mixer.

Figure 12: Schematics of an IQ mixer.

As shown before, the phase between the LO and RF is critical. In many applications this may be an undesired difficulty. To get around this problem, we may use an IQ mixer (In-phase - Quadrature). In this case, we use two mixers where between the two LO ports, there is 90° phase.

In this configuration, the magnitude and phase of the signal can be calculated from the voltage of the IF ports.

$$|\text{RF}| = \sqrt{\text{IF}_\text{I}^2 + \text{IF}_\text{Q}^2} \tag{13}$$

$$\text{phase} = \arctan(\text{IF}_\text{I}/\text{IF}_\text{Q}) \tag{14}$$

2.4   The studied materials

The capability to study materials at lower temperatures than before can be advantageous for many materials, but the increased magnetic field is only beneficial in some special cases. One of these is studying the ferromagnetic resonance (FMR) of some non-conventional samples.

FMR measures the bulk magnetization of the sample, because the individual electron spins are correlated. Although FMR is very similar to ESR, there are some important differences (as discussed in detail in [1]).

The magnetization of the ferromagnet in a given static field is much larger than the magnetization experienced in standard ESR measurements, where paramagnetic systems are studied. The shape of the sample plays an important part in the study of ferromagnetic materials, as it may cause the material to have a preferred magnetization direction.

FMR is generally much easier to measure and does not require the relatively complex setup like an ESR spectrometer, the increased absorption can be more directly observed. However for FMR signals reaching high magnetic fields are often important.

There are some samples however where the FMR signal is much smaller than typical, often due to their small size. The small effective size of a sample can be due to its shape.

Our colleges in Madrid are studying some interesting samples, like complex oxide

based ferromagnetic multilayers. Another type of interesting samples are ferromagnetic nanowires in alumina template (Fig. 13).
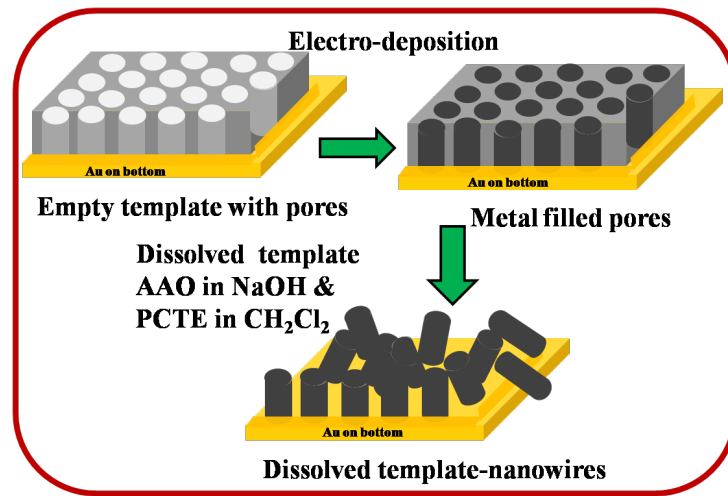

Figure 13: Example of the growth of ferromagnetic nanowires. From Ref. [6].

3 Results

3.1 The Madrid probehead

Our laboratory is participating in an ongoing cooperation with a solid state physics laboratory of Instituto de Ciencia de Materiales de Madrid, which is an institute of CSIC (Spanish National Research Council). A probehead was built using their instruments.

The cryostat and magnet available was a Physical Properties Measurement System (PPMS) from the company Quantum Design. The PPMS system is a versatile and easily automated for temperature and magnetic field dependent measurements. Its parameters:

- High magnetic fields are reachable up to $\pm 9\,\mathrm{T}$.

- Low temperatures down to a minimum of $0.5\,\mathrm{K}$, using a Helium-3 refrigerator.

- $25.4\,\mathrm{mm}$ diameter sample compartment with a flow-through design.

- Easily accessible electrical contacts at the bottom of the sample compartment.

A new loop-gap resonator was built to be incorporated in a probehead fitting in the PPMS sample chamber. To fit inside the sample chamber, the outer diameter of the shield is $25\,\mathrm{mm}$.

See Fig. 14 for a photo and Fig. 15 for an illustration of the probehead without the shield and Fig. 16 for the resonance curve. By fitting a Lorentzian on the curve, it can be calculated that the resonance frequency is $9.07\,\mathrm{GHz}$ and the quality factor of the resonator is 237.

The diameter of the shield is much smaller than the ones found in the literature, or the ones that have been previously tested. Due to this, the precise position of the loop-gap resonator, the couplers, the sample, and any other metal objects (like screws) greatly distort the electromagnetic field near the resonator and impairs its operation. So far no working method for magnetic modulation has been found, as placing any additional metal (eg. the cables for the modulator coils) made the resonator unreliable. The probehead was tested using the ESR spectrometer setup with the hybrid (see Fig. 3) and no successful measurements were made.

Other designs for resonators are being tested to suit the unusually small space available.

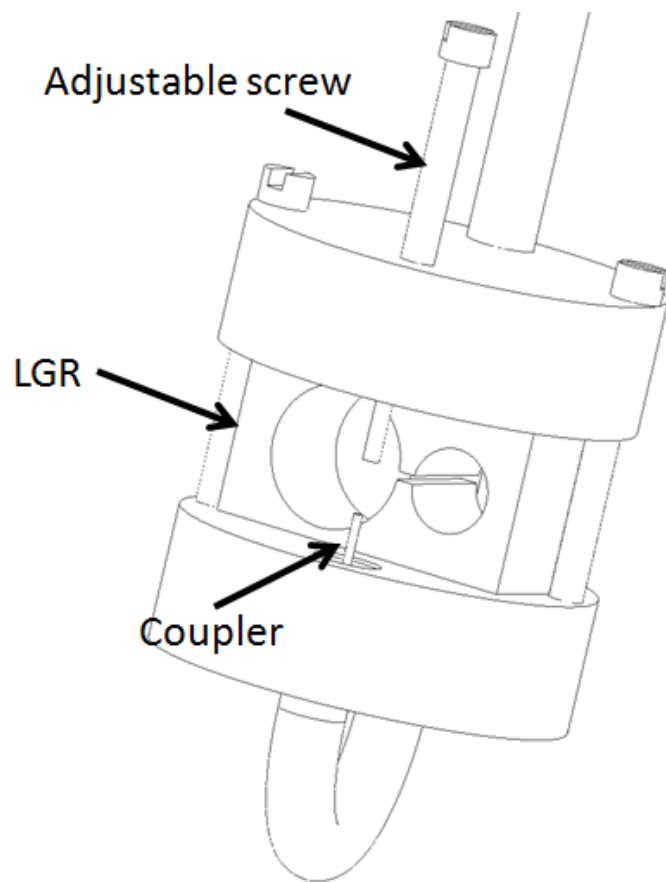Figure 14: Photo of the probehead built for the PPMS.

Figure 15: 3D model of the probehead built for the PPMS. The adjustable screw can be used to modify the coupling.
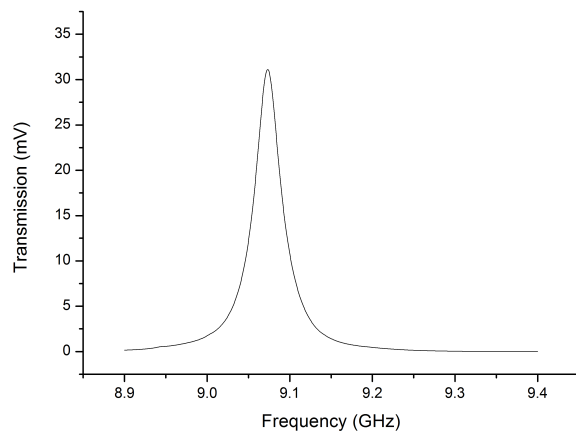

Figure 16: Resonance curve of the resonator measured in transmission.

3.2   The Budapest probehead

Using the instruments available in the ESR laboratory of the BME Physics Institute was more successful. The cryostat and magnet available was built by Cryogenic Ltd (London). Its parameters:

- High magnetic fields are reachable up to $\pm 9\,\mathrm{T}$, with $10\,\mathrm{ppm}$ homogeneity in its $55\,\mathrm{mm}$ long variable temperature insert(VTI).

- Low temperatures down to a minimum of $2\,\mathrm{K}$.

- $40\,\mathrm{mm}$ diameter sample compartment, with a flow-through design.

- The helium used for the cooling the sample is circulated in a closed loop.

Figure 17: The whole probehead that fits inside the cryostat.

See Fig. 18 for a photo and Fig. 19 for an illustration of the probehead without the shield and Fig. 20 for the resonance curve. By fitting a Lorentzian on the curve, it can be calculated that the resonance frequency is $9.64\,\mathrm{GHz}$ and the quality factor of the resonator is 114. As the coupling to the resonator in this measurement was critical, the uncoupled quality factor is about 228.

The space available in this probehead is much larger than in the Madrid probehead. Note that the coupler and cables are further away from the resonator, making this probehead more reliable. Also the magnetic modulation is outside the microwave shield, seperated by a thin metal plate.

See Fig. 17 for a photo of the whole probehead. Successful measurements were made using this probehead and the ESR setup with circulator (Fig. 2). The sample is placed in one of the loops of the loop-gap resonator. Since there is negligible electric field in the loop, the material of the sample holder (generally PTFE) does not disrupt the resonator, which is an advantage of this resonator design over the classic cylindrical cavity resonator.
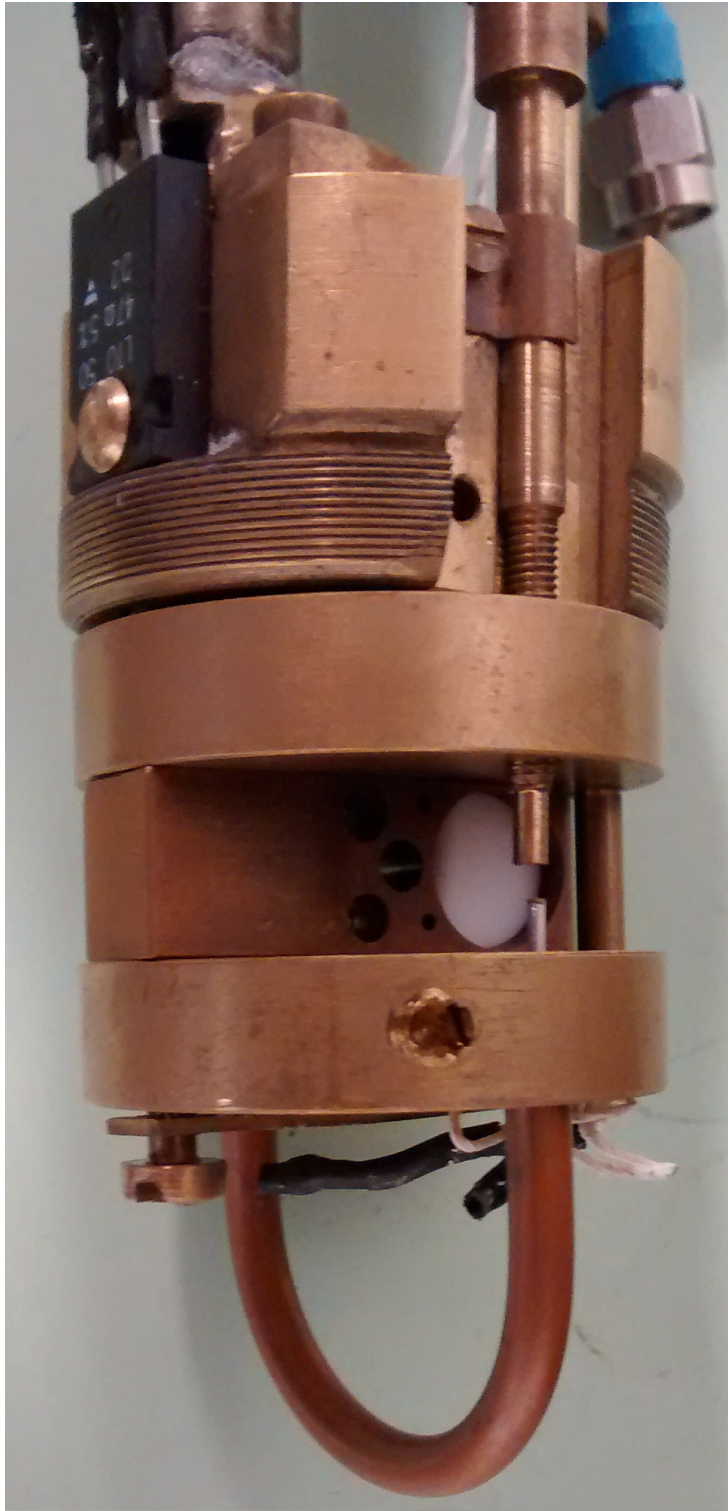
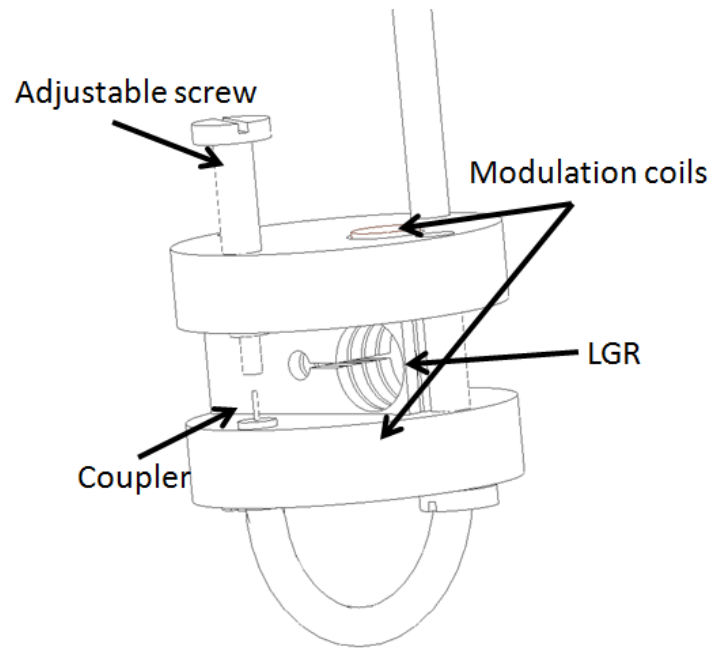Figure 18: Photo of the Budapest probehead.
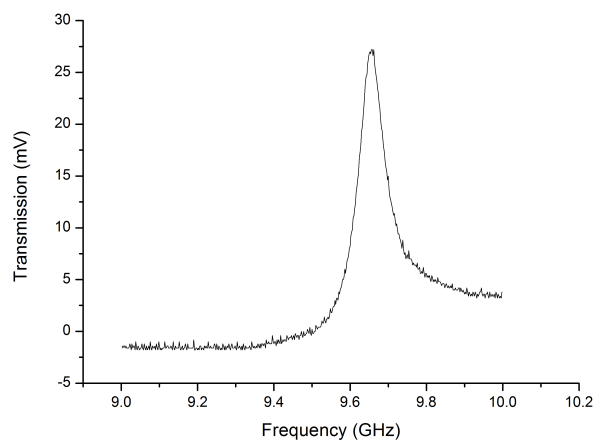
Figure 19: 3D model of the Budapest probehead.

Figure 20: Resonance curve of the resonator measured in transmission.

3.3   ESR measurements on DPPH

To compare the performance of a new ESR spectrometer to a commercial spectrometer, measurements on a standard samples are used. The standard is DPPH (2,2-diphenyl-1-picrylhydrazyl) is an organic powder. The DPPH molecule has a free radical per every molecule, so it gives a relatively large ESR signal, using small samples. The new ESR spectrometer is compared to a commercial Jeol X-band spectrometer using the same sample containing about 1 mg of DPPH.

Measurements made by the Budapest setup are presented and compared to measurements made by the Jeol spectrometer. The only modification of the presented setup is that an 100x IF amplifier was used between the mixer and the lock-in amplifier, as the noise of the mixer is about $2\mathrm{nV}/\sqrt{Hz}$, and the noise of the lock-in amplifier is about $8\mathrm{nV}/\sqrt{Hz}$. The signal of the DPPH proved to be too large, so the noise was always dominated by the digital noise. To still be able to provide a signal-to-noise ratio for each curve, the noise was separately measured by the lock-in amplifier.

The magnetic modulation amplitude can be measured by overmodulating a signal with a narrow linewidth (like that of the DPPH). By fitting a well-known curve to the overmodulated ESR spectrum, the magnetic modulation corresponding to each modulating current value can be calculated.
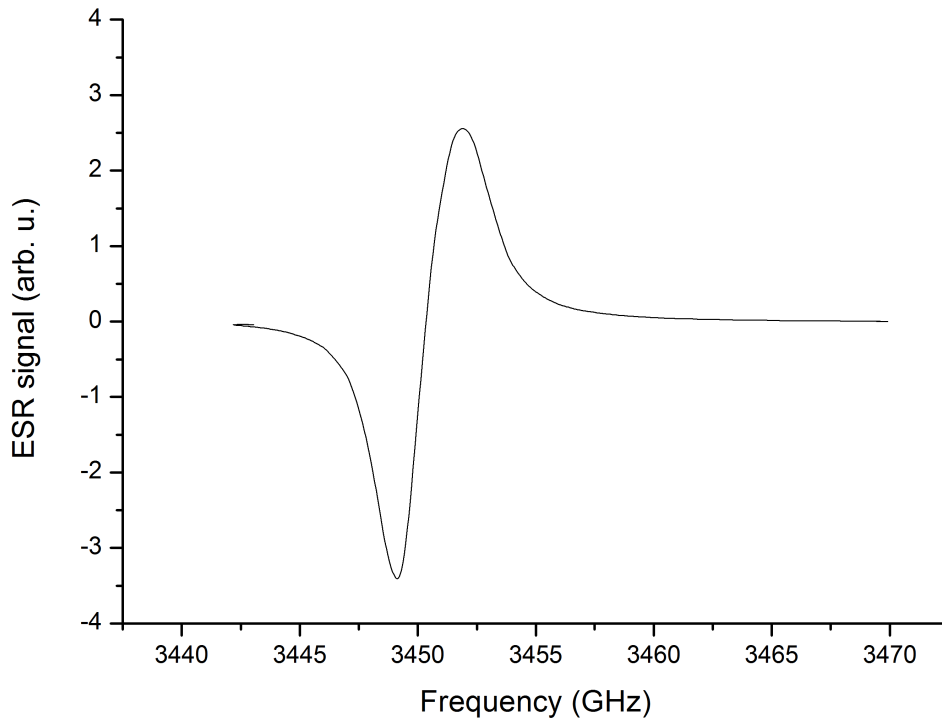

Figure 21: ESR spectrum measured by the Budapest probehead, using 0.5 G modulation.

See Fig.21 for a typical DPPH ESR spectrum.

Setup	Modulation	Signal	Noise	Signal-to-noise ratio
Budapest probehead	0.05 G	23 mV	275 nV	$8 \cdot 10^4$
Budapest probehead	0.5 G	220 mV	250 nV	$9 \cdot 10^5$
Jeol X-band spectrometer	0.05 G	1 V	7 μV	$2 \cdot 10^5$
Jeol X-band spectrometer	0.5 G	1.2 V	6 μV	$2 \cdot 10^5$

Table 1: Comparison of the new setup with a commercial available spectrometer.

See Table 1 for the comparison of the spectrometers. Note that for certain measurement parameters the new ESR setup gave better results than the commercial spectrometer. It should be understood that these results are not necessarily indicative of a future comparison for more difficult samples.

4   Conclusions

The work in this TDK thesis was motivated by the need for a novel type of ESR spectrometer: which allows the simultaneous use of cryogenic temperatures and non $g \neq 2$ resonance conditions. The motivation arose in a study of correlated magnetic systems (ferro- or antiferromagnetic) where such resonance conditions are common and where the interesting physical phenomena occur below 4 K.

It turns out that the variable temperature inserts of superconducting magnets are suitable to place the microwave resonators but it also limits the available room. This limitation was overcome by the design and manufacturing of so-called loop-gap resonators, which are lumped microwave elements.

I have built two electron spin resonance probeheads one to be used at the Instituto de Ciencia de Materiales de Madrid and another for use in the ESR laboratory of the BME Physics Institute. The use of loop-gap resonators yields additional benefits due to the higher filling factor, which is advantageous for small sized samples. I demonstrated the effectiveness of the Budapest probehead, work is still in progress on the Madrid probehead. I have shown using an ESR standard sample (DPPH) that the sensitivity of the home-built probehead approaches that of a commercial conventional spectrometer. I plan to continue the testing of the probeheads on scientifically relevant ferromagnetic samples.

5   References

References

[1] C. Kittel. *Introduction to Solid State Physics.* Wiley, 2004.

[2] C. P. Poole. *Electron Spin Resonance: A Comprehensive Treatise on Experimental Techniques.* Dover Books on Physics. Dover Publications, 1996.

[3] Gareth R. Eaton George A. Rinard. *Biomedical EPR, Part B: Methodology, Instrumentation, and Dynamics.* Springer US, 2005.

[4] J.S. Hyde W. Froncisz, T. Oles. Q-band loop-gap resonator. *Rev. Sci. Instrum.*, 57:1095–1099, 1986.

[5] http://cas.web.cern.ch/cas/Denmark 2010/Caspers/Skyworks-SchottkyDiodes-Basics

[6] Sachin Pathak Manish Sharma and Monika Sharma. *FMR Measurements of Magnetic Nanostructures, Ferromagnetic Resonance - Theory and Applications.* InTech, 2013.